



# Standard Nature of the Passive Layers of Buried Archaeological Bronze - The Example of Two Roman Half-length Portraits

Luc Robbiola, Loïc-Pierre Hurtel

## ► To cite this version:

Luc Robbiola, Loïc-Pierre Hurtel. Standard Nature of the Passive Layers of Buried Archaeological Bronze - The Example of Two Roman Half-length Portraits. METAL 95: International conference on metals conservation, Sep 1995, Semur-en-Auxois, France. pp.109-117. hal-00975718

HAL Id: hal-00975718

<https://hal.science/hal-00975718>

Submitted on 10 Apr 2014

**HAL** is a multi-disciplinary open access archive for the deposit and dissemination of scientific research documents, whether they are published or not. The documents may come from teaching and research institutions in France or abroad, or from public or private research centers.

L'archive ouverte pluridisciplinaire **HAL**, est destinée au dépôt et à la diffusion de documents scientifiques de niveau recherche, publiés ou non, émanant des établissements d'enseignement et de recherche français ou étrangers, des laboratoires publics ou privés.

## Standard Nature of the Passive Layers of Buried Archaeological Bronze

### The Example of Two Roman Half-length Portraits

L. ROBBIOLA and L.-P. HURTEL\*

Laboratoire de Métallurgie Structurale, ENSCP, 11 rue P. et M. Curie, F-75005 Paris.

\*Institut Français de Restauration des Œuvres d'Art, 1 rue Berbier du Mets, F-75013 Paris.

#### Abstract

Study of the patinas of two Roman half-length portraits has been conducted in order to improve our understanding of the corrosion processes according to a standard model of the Cu-Sn corrosion structure. The chemical and physical nature of the patinas has been characterized from sampling of corrosion products but also on metallic cross-sections of the artefacts, using complementary physico-chemical methods. The effect of decuprification of the alloy has been determined and the influence of the soil composition investigated.

#### Keywords

Cu-Sn alloy, passive layer, corrosion mechanisms, corrosion products, Roman portrait, authentication.

#### Introduction

Since the classical structure of corrosion developed by Organ [1], green copper II compounds with red cuprous oxide on the alloy, numerous studies have improved our knowledge of the nature of the patinas of archaeological bronzes of various historical periods [2-8]. They reveal several similar features, such as a high tin content in the corrosion products, an isomorphic alteration which preserves the original size of the artefact. In the general case of single phase Cu-Sn alloys (Sn weight% < 7-12), recent studies [9-11] have shown that the bronze patinas can be regarded as passive layers which can be described using a simple

model corresponding to a two-layer corrosion structure described by Figure 1:

- an outermost layer, characterized by high Sn/Cu ratios and by the presence of elements from the corrosive environment (such as O, Al, Si, P, Cl, Ca and Fe);
- an internal layer in contact with the alloy, irregular in shape and thickness, characterized by a lower Sn/Cu ratio than in the upper layer. The only detected element from the environment is oxygen. Sometimes this internal layer is not observed.

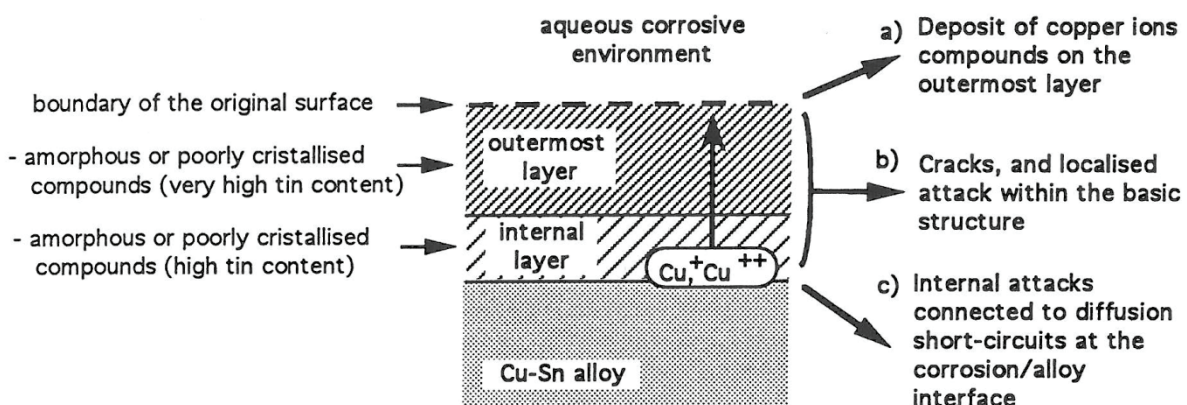


**Figure 1.** Schematic representation of the passive structure ("noble" patina) of bronze artefacts made from single-phase alloys, with the three groups of deviations: a) crust or deposit on the outermost layer, b) internal localised attacks within the passive layers and c) attack at the corrosion layers/alloy interface. Source: ref. [11].



**Figure 2.** Photographs of the two Roman half-length portraits of Livia and Augustus - Louvre Museum (both are 21 cm high and 11 cm wide).

The process of formation of this structure has been attributed to an internal oxidation of tin along with selective dissolution of copper from the alloy (decuprification). The growth of the patinas is controlled by the cationic migration of copper from the alloy to the external corroded surface. In several cases, some deviations can affect this standard model. As already shown in a previous work [11], these deviations can be classified into three groups as shown in Figure 1-right.

This model of patina together with its variations is fundamental in understanding the exact nature of the degradation of the artefacts and to diagnose the state of conservation.

The aim of this article is to characterize the passive layers, often called "noble patina" [8], in relation to this new standard model\*, using the example of two Roman bronzes representative of buried archaeological objects found in museums. The significance of the decuprification phenomena will be also discussed both in relation to the tin content in the alloy and to the influence of the soil.

## Roman Bronzes - Description and Characterization

### Description

The two bronzes (Figure 2) are the portraits of Augustus and Livia (the Roman Emperor and his wife-27 BC to 14 AD). They were discovered at the same place, by chance, in a sandy soil in 1870; the archaeological conditions were not adequately reported [12]. Since 1960, they have been conserved in the Louvre Museum. Portraits like these appear at the end of Greek antiquity along with significant worship of

political personality. Later this concept invades the whole of the Roman Empire, up to its distant provinces. The bronze portrait was the representation of character during the life time and a symbol of memory after death. Portraits were also used in political life and were brought by the Roman officials to the Provinces as a symbol of power. Portraits were also made for more humble Roman citizens (soldiers, people of middle class etc...).

### Surface Aspect

The surface conditions of Augustus' and Livia's portraits look very similar. They can be described as a lustrous, dark green, soft and homogeneous patina. Old restorations (mechanical cleaning) have induced scratches and in a few part a "wear" of the patina. An old wax protective coating was also clearly detected in some locations. Thick deposits of earthy crusts, however, remain on the outer surfaces on some parts of the heads (hair, ears, corner of the lips, etc...). On the inside, thick deposits of pale green products and earthy crusts were also present, but no apparent casting core was observed.

At low magnification (around x10), optical examination of the surface revealed dendritic patterns, corresponding to an as-cast bronze condition, with in very few places manifestations of localized corrosion such as pits or small crevices, often containing green products. The dendritic structure is equivalent to an etching of the surface revealing ghost dendrites, as mentioned by Oddy and Meeks [5]. So, the patina has the characteristics of a passive layer which preserves the original surface of the artefacts. This patina seems comparable to those observed on numerous buried archaeological bronzes either with a low or a high -tin content [2-11, 13, 14].

\* For language convenience, the passive layers due to corrosion processes will be identified in this text by the general term of "patina".

**Table 1.** Chemical composition of Roman statuary. Chemical analysis by UV emission spectrometry with a DC argon plasma source (weight %), Cu is the major element and has not been analysed.  
(1) = objects located at the Vatican Museum; others at the Louvre Museum.

Artifact	Year	Sampling	Sn	Pb	Zn	As	Sb	Fe	Ag	Ni	Bi	Co
Auguste	10 BC	chest	5.0	6.0	0.005	0.020	0.326	0.004	0.146	0.038	0.053	<0.001
		shank	5.2	7.0	0.014	0.039	0.411	0.253	0.152	0.050	0.003	0.002
		shoulder	4.3	5.1	0.011	0.016	0.307	0.004	0.142	0.038	0.009	<0.001
		base	5.7	5.8	0.010	0.022	0.350	0.004	0.156	0.046	0.005	<0.001
Livia	10 AD	chest	5.7	5.2	0.011	0.014	0.332	0.004	0.086	0.043	0.005	<0.001
		right plait	3.8	9.6	0.003	0.009	0.323	0.062	0.139	0.058	0.006	<0.001
		left plait	3.8	9.1	0.003	0.013	0.397	0.054	0.131	0.057	0.005	0.001
		base	5.7	5.0	0.008	0.017	0.310	0.004	0.160	0.040	0.005	0.001
Unknown	70 BC	chest	5.4	1.5	0.001	0.004	0.080	0.103	0.038	0.026	0.005	0.001
Unknown	10 AD	chest	6.0	4.5	0.036	0.033	0.057	0.069	0.034	0.056	0.005	0.004
		chignon	6.1	4.0	0.035	0.031	0.051	0.077	0.05	0.050	0.005	0.004
Gordien 3(1)	240 AD	neck(left)	5.8	14.6	0.505	0.519	0.082	0.342	0.048	0.020	0.003	0.001
		neck(right)	3.6	16.0	0.406	0.313	0.072	0.697	0.037	0.013	0.003	0.005
Pusio(1)	50 AD	neck	5.7	7.9	0.030	0.055	0.060	0.099	0.043	0.013	0.021	0.001
		left ear	6.2	4.4	0.006	0.033	0.057	0.026	0.036	0.014	0.003	0.001
Valens(1)	300 AD	tiara	2.1	17.7	0.073	0.082	0.101	0.099	0.069	0.046	0.006	0.004
		left eye	2.1	16.0	0.165	0.100	0.106	0.750	0.057	0.068	0.006	0.006
		ear	1.5	17.7	0.097	0.084	0.090	0.043	0.059	0.053	0.003	0.004
Tibere(1)	0	neck	4.5	10.2	0.004	0.112	0.204	2.6	0.041	0.045	0.003	0.005
Broken head(1)	160 AD	head	4.7	14.3	0.024	0.040	0.104	0.113	0.038	0.021	0.003	0.004
Fanciullo(1)	100 AD	left shoulder	1.9	16.0	0.001	0.031	0.092	0.025	0.042	0.030	0.003	0.001
		ear	4.2	15.2	0.017	0.026	0.085	0.083	0.040	0.028	0.027	0.001

### Metallurgical Characterization (Technology and Composition)

The optical examinations of the two pieces, followed by X-ray radiography, show that they are very similar from a technical point of view. Both were cast by the lost wax process as mentioned previously. Some core pins are still visible. Casting defects have also been detected. They are essentially gas porosities, mainly observed in the nape of Livia's neck. The thickness of the metal walls is from 3 to 5 mm.

Chemical composition of the alloys has been determined by UV emission spectrometry with a D.C. argon plasma source. Samples have been taken out by drilling in order to obtain about 30 mg of metal without corrosion. The alloys are leaded bronze

(Table 1), with an average content of 5.1% Sn and 6.0 %Pb for Augustus, and 5.7% Sn and 5.2% Pb for Livia (weight %). From the similar composition of the major elements and impurities (As, Sb, Fe, Ag, Ni, Bi and Co), both portraits were certainly poured at the same time

These two half-length portraits have been compared with other comparable Roman portraits from the collections of the Louvre Museum and the Vatican Museum [15]. All these objects are leaded bronzes (Table 1) cast by the lost wax process, and show in general a similar surface aspect. The variations of lead and tin contents in relation with the chronology (Figure 3) reveal that the lead content increases from the first century to the third AD, while the tin content remains constant.

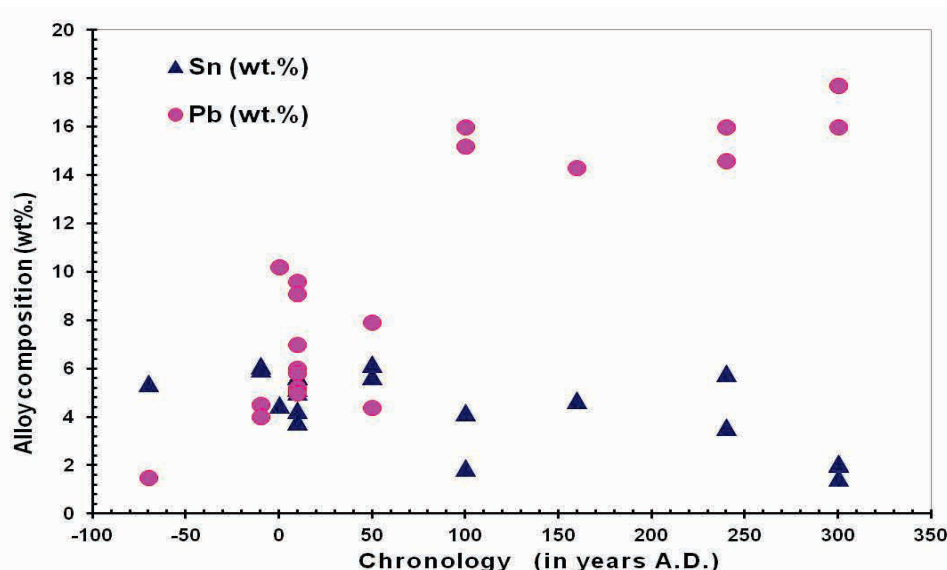


**Figure 3.** Evolution of the Sn and Pb contents of Roman artefacts (Table 1) in relation to chronology (A.D.)

**Table 2.** Elementary composition of the surface samples from Augustus and Livia's half-portraits. EDS analysis of the chemical elements for each samples were expressed as normalised ratios relatively to the copper amount (%weight) before the calculation of the mean values and the standard deviation.

(weight%)	P/Cu	Al/Cu	Ca/Cu	Si/Cu	Cl/Cu	Fe/Cu	Sn/Cu	Pb/Cu
dark green products	0.07± 0.03	0.03 ± 0.02	0.02± 0.02	0.12±0.05	0.01 ±0.01	< 0.01	1.2±0.3	0.3±0.2
green products	0.02 ± 0.01	0.08 ± 0.06	0.03 ± 0.03	0.23±0.2	0.01 ± 0.01	0.03±0.02	0.2±0.1	0.07±0.04
earthy crusts	0.03 ± 0.01	0.035 ±0.12	0.07 ± 0.05	1.0± 0.3	0.02 ± 0.01	0.19±0.07	0.1 ±0.1	0.02 ±0.02

Considering the history of metallurgy of bronze statuary, the earliest Greek statues were solid, but about 650 BC the lost wax process was introduced, probably from Egypt. In Europe, the Greeks and Etruscans must be credited with the first intentional addition of lead in bronze statuary either to improve the fluidity of the metal or to create the fine patina which is supposed to develop. Its effect on the corrosion resistance of bronze is, however, not well defined. Addition of lead to copper base alloys has occurred as early as the end of the Bronze Age; at low concentrations it could be intentional (due to assay or remelting process) or not. Only when the content is high could the addition of lead be considered deliberate and related to metallurgical uses. The Romans certainly adopted and extended the Greek discovery and added lead in statuary. They used leaded bronzes not only for statuary but also for general purposes: coins (the as dating from 5 BC contain 19-25 weight% lead) and engineering (typical engineering uses of leaded bronze were in pumps, stop-cocks, valves and other fittings for appliances used in supplying water).

It is well known that lead has only a limited miscibility in copper in the liquid state and is virtually insoluble in the solid state. The hardness and tensile properties of lead-tin-bronze depend much more on the tin content than on the lead content. The effects of lead, when present as a major alloying constituent in leaded bronzes (as an uniform dispersion of small particles of a soft dense metal throughout the stronger bronze matrix), are a gradual linear reduction of tensile strength, elongation, hardness and a gradual increase in density. Machinability is improved (the lead content causes complete shearing of the chips during machining, assists lubrication and tends to keep the tool cool) but resistance to wear and deformation are lessened.

Due to these properties, the Romans used this alloy for mass production and also to produce pieces which could reach large size, and required much assembly and finishing. Lead was not expensive so it can be intensively extracted from easy to locate ores. Its production also increased with the strong development of silver production by cupellation.

From these results, it appears that the composition of the two half-length portraits represents an important facet of Roman metallurgy.

## Patina - Composition and structure

### Experimental procedure

In order to determine the chemical nature of the patina,

the microsamples were taken off mechanically by scraping the corroded surfaces gently with a very fine tungsten needle.

According to surface optical examination, the corrosion product samples can be classified into three groups:

- dark green products corresponding to the patina;
- green products of supplementary outer products (corresponding to case a of Figure 1);
- earthy crust deposits on the corroded surface (also described in Figure 1).

As mentioned previously, these patinas would be due to a depletion of copper (decuprification). The earthy crusts could thus be regarded as soil "contaminated" (corroded) by copper ions stemming from the dissolution of the alloy. It is the reason why earthy crusts (soil products) with corrosion products just beneath were also particularly considered in this work.

The microsamples were analysed by X-ray energy dispersive spectrometry (EDS) mounted on scanning electron microscope (SEM). Identification of the chemical compounds was made by X-ray diffraction and by infrared spectrometry. Infrared spectrometry was conducted by crushing microsamples in CsBr, with 3 mm pellet diameter, in a corundum ( $\alpha$ -Al<sub>2</sub>O<sub>3</sub>) mortar in order to avoid contamination, because the corrosion products may have a higher hardness than 6 Mohs and scratch an agate mortar. It already appeared that other compounds than the usual copper products described in the literature are present: tin-oxide or -hydroxide products in the corrosion layers, known to have a high hardness, were also expected. The presence of tin-oxide species will be confirmed later.

To provide more information on the internal structure of the patina and the alloy, metallographic examinations have also been carried out. Two small fragments of the half-portraits were taken out for this purpose.

### Results

The two bronzes have the same nature of patina (composition and microstructure).

The elemental analysis of the whole surface samples distinguishes three clusters of patina products, well defined according to the three groups of compounds previously described. Average compositions with standard deviations are given in Table 2 for each of them. Results, summarized in Figure 4, show that:

- the dark green products, the basic constituents of the patina, contain a very high proportion of the alloy elements (Sn and Pb) with soil elements.

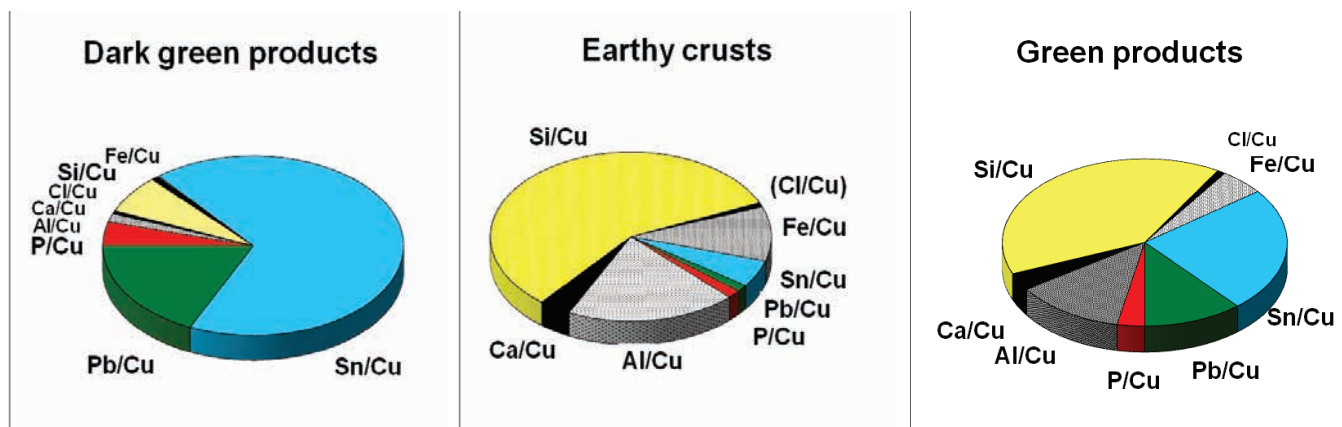


**Figure 4.** Relative chemical composition (% weight ratio) of the surface compounds scraped mechanically off the bronze of Augustus' and Livia's half-portraits. Values from Table 2.

Phosphorus, silicon and aluminium are high, while the others, such as calcium, chlorine and sulfur, are present only in very low amounts. These soil elements are in fact common constituents in the passive layers of ancient bronzes and their nature and amount modify the colour of the patina [16].

- the green products are mainly copper corrosion products described on ancient bronzes buried in soil.
- the earthy crusts contain high amounts of Si, Al and Fe and lower amounts of Ca, P and Cl. They are characteristic of a clayey sand [17]. They contain Cu and also very low amounts of Sn and Pb. The ratios Sn/Cu and Pb/Cu are very low, due

to the fact that copper ions are the main cationic metallic species which have diffused into the soil, while Sn and Pb cations have not.

X-ray diffraction analysis showed copper hydroxy-carbonate (malachite) in green corrosion products and no crystalline compounds in all patina samples which correspond to the dark green products. They are amorphous mineral compounds and correspond well to the classical schema of the standard model (Figure 1).

X-ray diffraction has often been used to identify corrosion products, but in this case infrared spectrometry has given more helpful results. Infrared spectroscopy clearly distinguishes the compounds

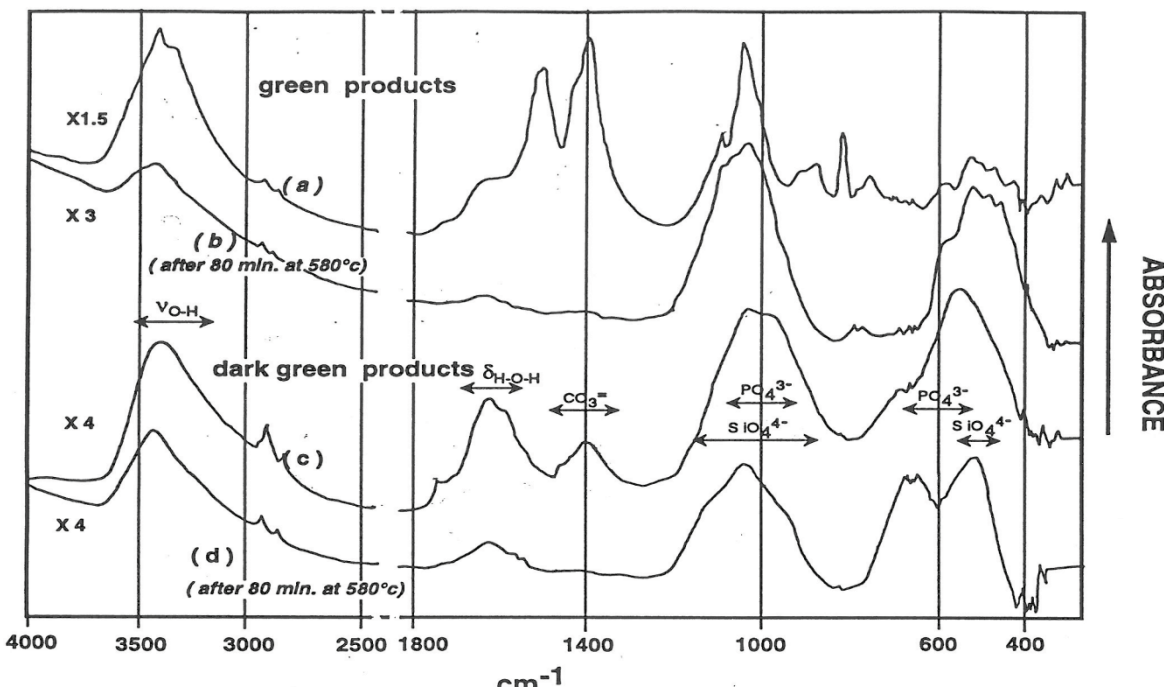


**Figure 5.** Representative infrared absorption spectra of a green corrosion product (a) and (b), which consists of copper (II) hydroxycarbonate compounds, and of a dark green product (c) and (d), which contains amorphous compounds (very broad bands) with probably hydrated silicate(s), phosphate(s), carbonate(s) compounds and metal oxides. The large band at 1650 cm<sup>-1</sup> - spectra (a) and (c) - is characteristic of water presence in the minerals compounds. It disappears after heating the pellets - spectra (b) and (d).

of the green corrosion products from those of the dark green patina (Figure 5). The green products (Figure 5a) are mainly hydrated copper carbonate hydroxide (hydrated malachite,  $\text{Cu}_2\text{CO}_3(\text{OH})_2\cdot\text{H}_2\text{O}$ ) with hydrated copper orthosilicate, according to natural corrosion compounds. In comparison to the well known pure malachite, hydrated malachite shows the following differences: a broad medium band on the 1600-1650  $\text{cm}^{-1}$  range due to the H-O-H bending mode, and a lower broad medium band on the 750-1100  $\text{cm}^{-1}$  range. The presence of silicate compounds was indicated by heating the pellets for 1 hour in a furnace at 580°C. As shown in Figure 5b, carbonates and hydrates are destroyed. Copper(II) orthosilicate compound with

probably aluminium silicate is the only one observed [18]. The dark green products (Figure 5c) are mainly amorphous orthosilicate and orthophosphate compounds combined with hydrated metallic oxides and some carbonates. After heating at 580°C (Figure 5d), a broad band at 600-680  $\text{cm}^{-1}$  appears. It could correspond to the formation of stannic oxide ( $\text{SnO}_2$ ) and probably cuprous oxide ( $\text{Cu}_2\text{O}$ ). Furthermore it is interesting to note that neither hexahydroxystannate ( $\text{Sn}(\text{OH})_6^{2-}$ ) compounds were found (no bands in region 650-850  $\text{cm}^{-1}$ ) nor mixed metallic oxides such as  $\text{CuSnO}_3$  [18]. So the hydrated metallic tin compounds could be mainly an amorphous hydrated stannic oxide ( $\text{SnO}_2\cdot\text{nH}_2\text{O}$ ).

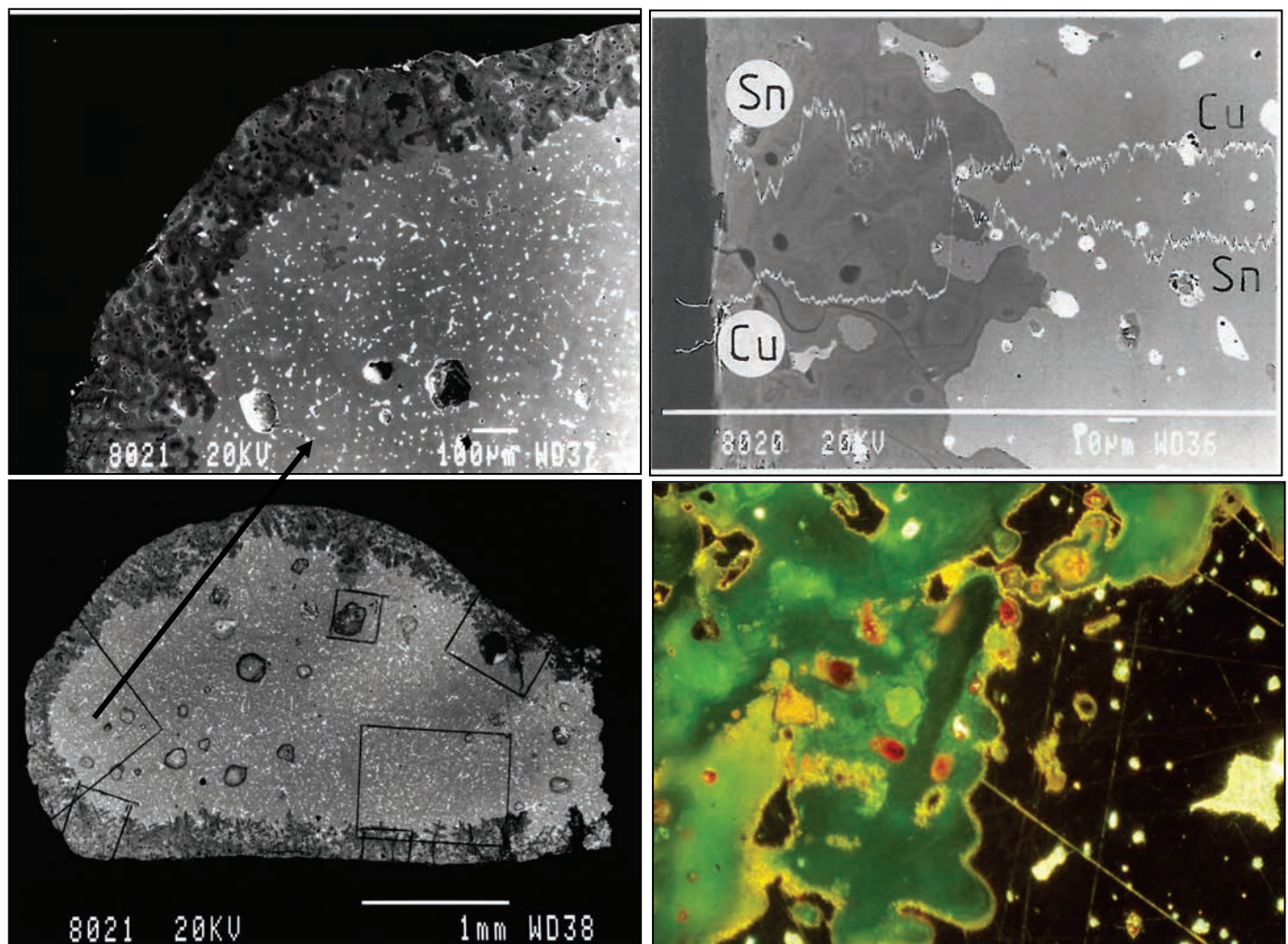


**Figure 6a left, 6b right (up):** Transverse microstructure of the cross-section from Augustus.

In Figure 6a, the uncorroded alloy (to the right) is a cast bronze containing lead globules (in white). The surface corrosion zone is to the left (in grey). The corroded compounds preserve the original structures well. Ghost dendrites and lead inclusions (in black) are observed.

In Figure 6b, x-ray intensity profiles of copper (Cu) and tin (Sn), corresponding to the white linescan, reveal clearly that a selective depletion of copper is observed in the patina. SEM-BEI.

**Not in the published version: Figure 6c left, 6d right (down)** – In Figure 6c (left): General vision of the cross-section of the Augustus's base: uniform corrosion is typically related to dendritic alpha phase alteration – corrosion thickness between 40 to 200  $\mu\text{m}$ . In Figure 6d (right) (image full scale ~250  $\mu\text{m}$ ): Optical dark field microscopy: patina/corrosion Interphase: corroded dendritic structure is in green (related to Cu(II) species) while bulk alloy is in black including white lead globules. Here no internal layer is clearly observed (only a "yellow" interphase is observed). Red inclusions in the green patina are related to Pb corrosion).

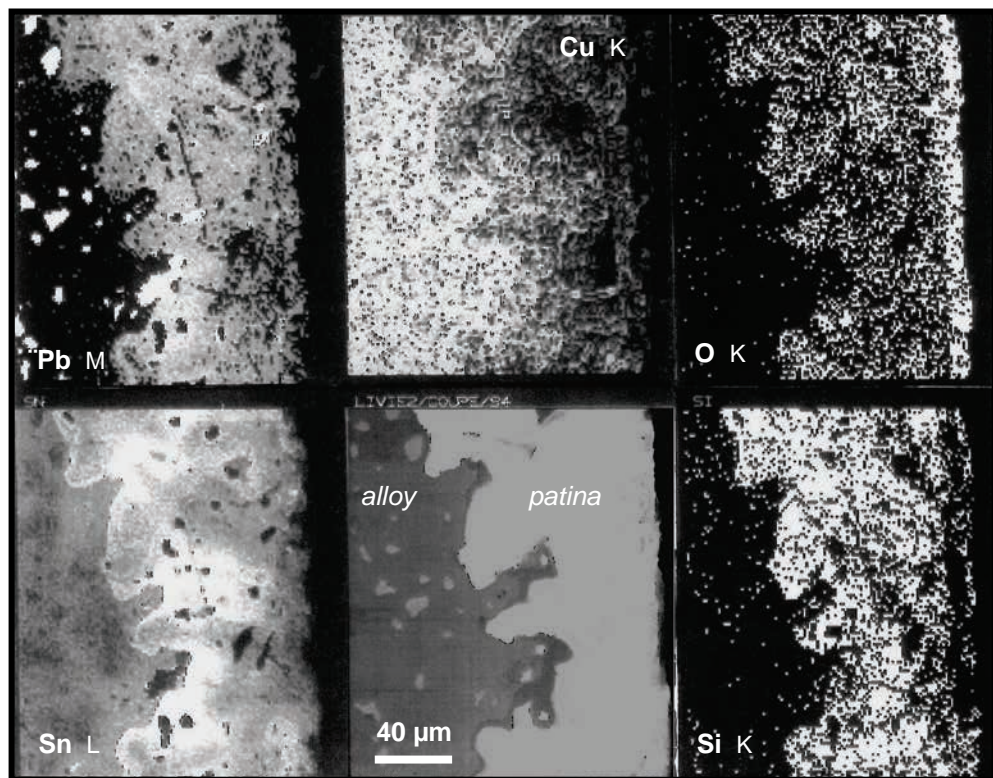


**Figure 7.** Transverse microstructure of the dark green patina from the cross section of Livia. Digital X-ray maps of the uncorroded alloy (left) and the surface corrosion zone (right, in white here)). Left to right, top to bottom: Pb, Cu, O, Sn, secondary electron image (SEM-SEI) and Si.

Structural examinations of the metallographic samples (Figures 6a,b) reveal the pseudomorphic structure of an as-cast alloy: "ghost" dendritic structure is generally continuous with the matrix of the uncorroded alloy. The thickness of the corrosion layer is in the range of 40 up to 200  $\mu\text{m}$ . The strong structural relationship between unattacked alloy and surface corrosion zone confirms the fact that the patina is due to an internal oxidation of the alloy with copper depletion (Figure 6b). The internal layer, described in the standard model in Figure 1, has, however, not often been observed. It could be probably related to the dendritic structure which allows a better diffusion of species into the grain than for an annealed single-phase alloy.

Analysis of the cross-sections by EDS confirmed that the corroded zone has the same chemical composition as the dark green scraped products previously characterized. Representative digital X-ray maps of Cu, Sn, Pb, O and Si are given in Figure 7, revealing the distribution of these elements in the patina. The corroded surface has a very low copper content and relatively high contents of the other elements. The copper and tin compositions have a tendency to follow dendritic microsegregation. As previously mentioned, lead is not miscible with the copper-tin solid solution. It forms white globules in the alloy (Figures 6a,b and 7), while, as has also been observed by other authors [4, 6], lead ions have diffused widely in the corrosion zone. The other elements are also quite uniformly distributed in all of the thickness of the patina. It is important to note that chloride ions are

always present throughout the patina, in weak concentration. However, in the case of "noble" patina, chlorides must be considered as being in a passive state and not playing a role such as in the case of the bronze disease when cuprous oxide is present [9].

## Discussion

From the whole examinations of the patinas of the two bronzes patina, it clearly appears that the passive surfaces, coloured dark green, are not made up of pure copper compounds. These "noble" patinas contain very high amounts of tin products, probably hydrated stannic oxide [8,14], which have a high chemical stability in a large pH range and in the lack of organic or complexing species in the corrosive environment [9]. They are also characterized by a strong enrichment from the soil compounds. In fact, the patina structure of these representative Roman bronzes agrees well with the standard model described in Figure 1, even though an internal layer of metallic oxide without soil elements is not observed due probably to the as-cast condition of these two bronzes.

Thus, with this new understanding of the corrosion processes [8-11,16], it can be assumed that the patina formation, by which both half-length portraits have undergone a pseudomorphic corrosion structure, appears as characteristic of the corrosion of a Cu-Sn alloy in a natural and moderately aggressive medium (pH range between 4 to 8.5) [17]. These patinas are the result of a decuprification of the alloy related to an

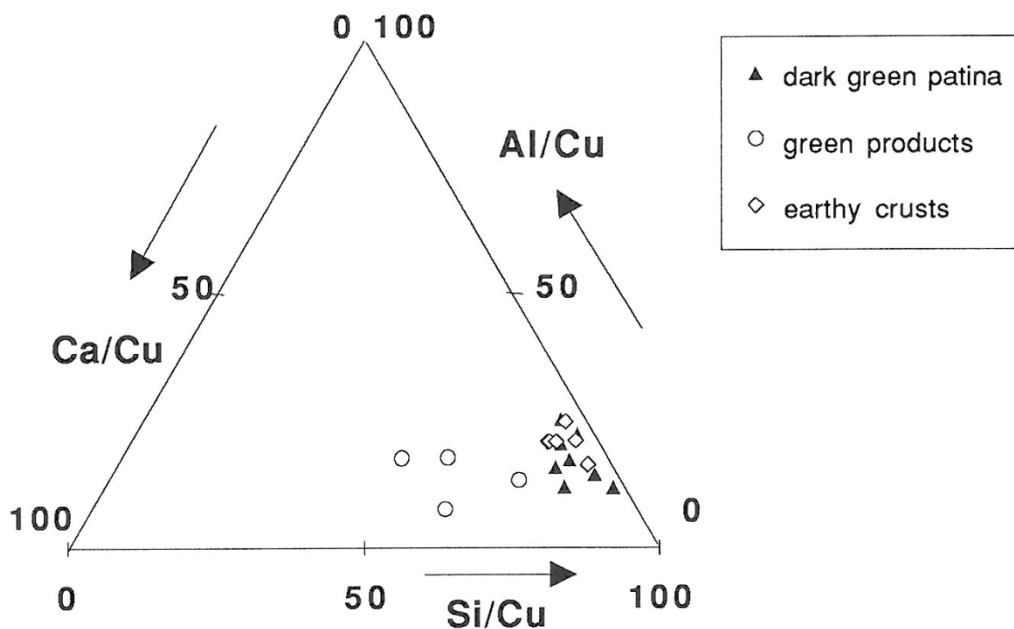


**Figure 8.** Plot of the chemical amounts of the scraped patina samples (dark green, earthy crusts and green products). Ternary diagram (Al/Cu, Si/Cu, Ca/Cu in weight% ratio)

internal oxidation. Copper is depleted from the alloy throughout the surface and the process is under the control of the migration of the copper ions, while tin compounds remain to preserve the structure. With the copper depletion, soil species (silicates, phosphates ...) have penetrated into the corrosion layers. Such a patina corresponds well to a very natural amorphous material, very protective against corrosion as already determined elsewhere by Soto et al. [19].

Consequently, such a stable corroded surface is also able to act as a physical and chemical barrier between the alloy and the corrosive environments. Indeed, during the patina growth in the soil, the rate of corrosion tends towards a zero limit. This can be reached when migration of the copper ions became strongly limited, *i.e.* when the thickness of the corrosion layers is sufficient to block the ions diffusion physically. For this reason, patina growth is not linear with time. It can be estimated that the necessary time to build up such a patina is of the order of a few hundred years if we postulate a mean corrosion rate of 0.5 µm/year [17]. So we can assume that the patina has been formed in a relatively "short" period of time after the burial in comparison to the whole burial time. These passive layers must be regarded as mainly due to the burial conditions. For this reason, two points can be stressed in order to give a new understanding of the nature and formation of patinas on ancient bronzes. These two points can also be considered as new data to determine a natural patina.

First, the amount of copper dissolved into the soil could be considered as a chemical-physical attempt of the alloy to reach a steady state in the corrosive environment: the more aggressive the environment is, the more copper will be dissolved. As already defined [10,16], the stationary state in a burial condition can be defined by a dissolution ratio  $\beta$  relative to the tin

fraction remaining in the outermost layer of the patina (the indexes  $p$  and  $a$  mean respectively *passive layer* and *alloy*) :

$$\beta = \frac{\left\{ \frac{\text{Cu}}{\text{Sn}} \right\}_a}{\left\{ \frac{\text{Cu}}{\text{Sn}} \right\}_p}$$

In fact it appears that the  $\beta$  factor is fairly constant for a given corrosive environment, independent of the tin content in the single-phase alloy. The  $\beta$  factor value will be high when the environment is more corrosive, *i.e.* when the copper dissolution is more important. In the case of moderately aggressive conditions, such as in a clayey-sandy soil, the ratio has been found to be:  $\beta=18 \pm 4$  [10]. This equation applied to the half-length portraits of Augustus and Livia gives:  $\beta = 19 \pm 8$  with  $\left\{ \frac{\text{Cu}}{\text{Sn}} \right\}_a = 17 \pm 2$  and  $\left\{ \frac{\text{Cu}}{\text{Sn}} \right\}_p = 0.9 \pm 0.3$  which is in good agreement with previous results on bronze patinas from various historical periods. Thus in our case, there is a good certainty that in these two Roman portraits, patinas are due to natural corrosion in a clayey sandy soil. The lead seems to have no direct influence on the copper selective dissolution of the matrix, probably related to the fact that lead is not miscible in the alloy and can be regarded as inclusions in the alloy matrix.

Secondly, we have examined the influence of the soil elements, considering that a chemical equilibrium has been reached between the patina and the soil. Due to the migration process of copper ions from the alloy and the penetration of soil species into the corroded surface zone, we may admit that the corrosion products reveal the imprint of the type of soil in which the bronze has been buried.

To verify this assessment we have plotted, in Figure 8, the chemical composition in soil elements (Al/Cu, Si/Cu and Ca/Cu) of both the corrosion products (dark green) and of the earthy crusts. Thus it shows a good correlation between the patina and the soil crusts: the patina was formed in a buried condition in a clayey sandy soil. Consequently, this confirms the fact that the earthy crusts on a bronze patina can be viewed as an "alteration" of the soil by the alloy.

## Conclusion

The study of the two half-length portraits of Livia and Augustus is rich in information. We showed from this study that two bronze artefacts with the same composition and metallurgical condition, buried in the same ground, present the same nature of patina. The passive layers (patina) can be described by a standard model in relation to decuprification of the Cu-Sn alloy related to an internal oxidation. A general understanding of the corrosion processes is now available to aid understanding of the corroded structures of ancient bronzes.

In this article, we also showed two phenomena: first, the dissolution factor of copper appears dependent of the chemico-physical steady state reached between the alloy and the corrosive environment; second, a patina contains the chemical imprint of its corrosive medium, making it necessary to take precautions in restoring and conserving the artefacts.

Applied to the study of works of art, these two phenomena appear to be two necessary criteria to authenticate a bronze, but they are not sufficient; knowledge of the alloy composition remains a necessity to check the accuracy of the patina analyses.

These general appraisals of the nature of the patina reveal the complexity of the corrosion processes. Further investigations are still necessary not only to complete our knowledge of the corrosion and the conservation state, but also to gain more on the information contained in these passive layers which could, then, be applied to define criteria of authentication.

## Acknowledgments

The authors would like to thank Mme Kate de Kersauson and M. Baratte, Curators, for showing interest in this research on the corrosion of bronze artifacts, and also the Laboratoire de Recherche des Musées de France where the main part of the study was done. We would also like to thank Mlle Laurence Garenne-Marot and Dr Tom Chase for their helpful comments on this text.

## Bibliography

1. R. M. ORGAN, "Aspects of bronze patina and its treatment", Studies in Conservation 8 (1963), 1-9.
2. R. F. TYLECOTE, The effect of soil conditions on the long-term corrosion of buried tin bronzes and copper, Journ. of Archaeo. Science 6 (1979) 345-368.
3. E. MELLO, P. PARRINI, E. FORMIGLI, Alterazioni superficiali dei bronzi di Riace , le aree con patina nera della statua A, in Due Bronzi di Riace, Bolettino d'Arte, special issue n°3 / I, 1982, 147-165.
4. M. SAWADA, Composition et corrosion des bronzes anciens - variations des teneurs des éléments principaux entre les couches de corrosion et l'alliage de base, in Nara Kokuritsu Bunkazai Kenkyusho, Bull. of the 30th anniversary, Nara Cultural Properties Research Institute, Japan, march 1983, 1221-1232 (in japanese).
5. W. A. ODDY, N. D. MEEKS, "Unusual phenomena in the corrosion of ancient bronzes", in Sience and Technologies, IIC Washington Congress, N. S. Brommelle & G. Thomas Ed., 1982, 119-124.
6. C. P. SWANN, S. J. FLEMING, M. JAKSIC, Recent applications of PIXE spectrometry in archaeology I. Characterization of bronzes with special consideration of the influence of corrosion processes on data reliability", Nucl. Instr. and Meth., B64 (1992) 499-504.
7. E. ANGELINI, P. BIANCO, F. ZUCCHI, On the corrosion of bronze objects of archaeological provenance, in Progress in the understanding and prevention of corrosion, Costa J. M. and Mercer A. D. Ed., The Institute of Materials Publ., vol. I (1993) 14-23.
8. R. J. GETTENS, Patina noble and vile, in Art and Technology : A symposium on classical bronzes, MIT Press, Cambridge MA, S. Doebringer, D.G. Mitten and A. Steinberg Ed. (1970) 57-72.
9. L. ROBBIOLA, C. FIAUD, Apport de l'analyse statistique de la composition des produits de corrosion à la compréhension des processus de dégradation des bronzes archéologiques, Revue d'Archéométrie 16 (1992) 109-120.
10. L. ROBBIOLA, C. FIAUD, Corrosion structures of long-term burial Cu-Sn alloys - Influence of the selective dissolution of copper, International Symp. on Copper and Copper alloys Oxidation, Rouen, July 1992, Mém. Et. Scien. Rev. Métallurgie Ed., Paris , n°6 (1992) 157-162.
11. L. ROBBIOLA, C. FIAUD, Basic structure of passive layers of Cu-Sn alloys applied to patinas of archaeological bronzes, Electron Microscopy 1994, ICEM 13 Paris, Les Editions de Physique Ed. (1994) 1261-1262.
12. M. BERTRAND, Procès verbal de la découverte de deux bustes en bronze d'Auguste et de Livia à Neuilly-le-Réal (Allier), Bull Soc. d'Emulation du Dpt de l'Allier, 1870, 255-258.
13. R. J. GETTENS, Tin-oxide patina of ancient high-tin bronze, Bulletin of the Fogg Museum of Art, 11 1 (1949) 16-26
14. N. D. MEEKS, Surface studies of Roman bronze mirrors, comparative high-tin bronze Dark Age material and black Chinese mirrors, in Proceedings of the 26th Int. Archaeometry Symposium, University of Toronto, May 1988, Farquhar R. M. et al. Ed., The Archaeometry Laboratory (1988) 124-127.
15. L. P. HURTEL, Analyse de la demi-statue et du portrait de Trebonianus Gallus appartenant au Musée du Vatican, in Bollettino Monumenti Musei e Gallerie Pontificie, vol. VIII, 1988, 52-53.
16. L. ROBBIOLA, C. FIAUD, A. HARCH, Characterization of passive layers of bronze patinas (Cu-Sn alloys) in relation with the tin content in the alloy, in Modifications of Passive Films, Europ. Fed. of Corrosion, n° 12, The Institute of Materials, P. Marcus, B. Baroux & M. Keddam Ed., (1994) 150-154.
17. M. ROMANOFF, Underground Corrosion, NBS Circular no 579, Washington DC, 1957.
18. R. A. NYQUIST, R. D. KAGEL, Infrared spectrum of inorganic compounds ( $3800-45 \text{ cm}^{-1}$ ), Academic Press Inc. (1971).
19. L. SOTO, J. P. FRANEY, T. E. GRAEDEL, G. W. KAMMLOTT, On the corrosion resistance of certain ancient Chinese bronze artifacts, Corrosion Science 3 (1983) 241-250.

## Résumé

*Afin d'améliorer la compréhension des processus de corrosion, l'examen des patines de deux bustes romains a été conduit en appliquant un nouveau modèle standard de la structure de la corrosion des alliages Cu-Sn. La nature chimique et physique des patines a été caractérisée à partir de prélèvements de produits de corrosion mais aussi à partir de coupes métallographiques des bustes, à l'aide de méthodes de caractérisation physico-chimiques complémentaires. L'effet de l'appauvrissement en cuivre de l'alliage a été démontré et l'influence de la composition du sol évalué.*